



# Machinability Investigation on Novel Incoloy 330 Super Alloy using Coconut Oil Based SiO<sub>2</sub> Nano fluid

Aniket Roy Choudhury<sup>1</sup>, Ramanuj Kumar<sup>1\*</sup>, Ashok Kumar Sahoo<sup>1</sup>, Amlana Panda<sup>1</sup>, Arunjyoti Malakar<sup>1</sup>

<sup>1</sup>School of Mechanical Engineering,  
KIIT Deemed to be University, Bhubaneswar, Odisha, INDIA.

\*Corresponding author

DOI: <https://doi.org/10.30880/ijie.2020.12.04.014>

Received 23 September 2019; Accepted 30 November 2019; Available online 30 April 2020

**Abstract:** Over the years, the quality of the finished surface has become the foremost prevalent owing to better output performance, reliability and life span of a machined part. Moreover, the effects of the cooling and lubrication approach during the machining process play a vital role. Incoloy 330 generally used in petrochemical, chemical, power generations and thermal processing applications. As this alloy has wide applications in diverse industries, however, its machinability behavior must be investigated for the manufacturing concern. Till today, no work has been reported on machinability of Incoloy 330 alloy. Considering this gap, the current work focuses on the appropriate utilization of the Minimum Quantity Lubrication (MQL) based cooling approach using diverse concentrations of coconut oil-based SiO<sub>2</sub> nanofluids in the turning practice of Incoloy 330 alloy. The input variables are nanofluids concentration (Nc), feed (f) and cutting speed (Vc). The cutting insert TiAlN PVD coated cemented carbide tool is utilized to study the output responses like tool flank wear (VBc), surface roughness (Ra), material removal rate (MRR), and chip morphology. SiO<sub>2</sub> nanofluids work effectively as tool flank wear is found to be less (VBc varies in between 0.057 mm to 0.077 mm). From ANOVA, cutting speed is found to be topmost influencing input (83.24%) for tool flank wear. Machining on the highest feed value (0.35 mm/rev) is not recommended for this work as Ra is found to be greater than 1.6 μm. With increasing cutting speed and feed rate, MRR increases. In each run, coiled continuous helical chips are obtained. Deformed chip thickness is found to be lower (0.3 to 0.74 mm) due to the application of SiO<sub>2</sub> nanofluid through MQL which enhanced the heat dissipation thus eliminated the tendency of chip welding on the top surface of the tool. Chip reduction coefficient decreases with feed and cutting speed. Further, the TOPSIS optimization technique has been implemented to get an optimum set of cutting parameters for multiple responses and it is found to be Nc3 (0.3 % wt)-f1 (0.15 mm/rev)-Vc3 (160 m/min).

**Keywords:** Incoloy 330, Nanofluids, MQL, Flank wear, Surface roughness, Chip morphology, TOPSIS

## 1. Introduction

Machining processes are illustrious in the manufacturing sector owing to their capability to manufacture close tolerances and high dimensional precision while concurrently maintaining the cost-effectiveness with more production outputs. Machining of Nickel-based super-alloy has attracted extensive attention due to their more hardness, more strength at higher temperature, lesser thermal diffusivity and affinity to react with the cutting tool materials [1]. In recent years, the focal objectives of production industries are to provide maximum production rate with the better-quality demand in machining practice to sustain in the competitive manufacturing market predominantly for the application in the nickel-based super alloy materials. Various factors impairing the output performance for nickel-based alloys, shorter tool span and rigorous surface exploitation of machined surface are the significant contemplations. Moreover, coolant plays a key role during cutting of nickel-based alloys. The use of coolant will reduce the

temperature of the machining region and the procedure of induced fatigue [2]. Environmental friendly methods during the machining of 7075-T6 aluminum alloy for automotive advantages have been reviewed [3]. Recently, jatropha oil bio-based lubricant has been developed that provides a suitable substitute to the world-dominating mineral oil-based fluids for sustainable and greener working surroundings [4]. The development of the analysis of nanofluids, such as the fabrication process, mechanism of stability assessment, stability improvement, nanofluids thermophysical characteristics have been summarized [5]. Further, the addition of 0.25% nano aluminium oxide in coconut oil leads to improve the thermal conductivity. Accordingly, it resulted the noticeable performance of the heat transfer rate [6]. The use of surfactant is the major driver of nanofluid performance improvement [7].

Meanwhile, many difficulties arise during the machining of hard-to-cut materials like the development of cutting tool wear that leads to shorter tool span, increase in machining cycle time and production of higher temperature at the work piece-tool flash that cardinally influences the properties of a machined surface [8]. With the aim of minimizing the consequences of high cutting temperature, proper use of lubrication during machining is very essential. Further, it has been summarized that for achieving the superior surface finish and lesser tool wear use of lubrication plays a significant role during machining [9]. Since a few years, there is widespread research going on in the field of Metal Working Fluids (MWFs) in machining sectors. Manufacturers are constantly trying hard to choose the best alternative of lubricants which is economical and ecological for machining concern [10,11]. The traditional use of coolants at some phases in the production process produces abundant technological and environmental issues. Easy removal of lubricating agents and coolants on conventional machining fluids may provide a better and efficient solution in the manufacturing sector where the depth of cut is more during machining without the use of lubricating [12]. Furthermore, MQL (Minimum Quantity Lubrication) technology has emerged into the machining sector for cooling and lubrication purposes. It has been observed that the usage of MQL has enhanced the performance of the machining fluids and less energy has been consumed during cutting operations (Ali et al. 2018). MQL technology has significantly improved the supportive surface roughness, minimized tool wear and chip formation during machining. It also assists in reducing the average tool-chip flash temperature by 10% and outperformed as compared to wet machining [13].

To improve the machining fluids performance, nano lubricants are added in several concentrations for better machining approach. Nano lubricants are the combination of nanoparticles, base fluids (Cutting fluids) and the dispersant. High-temperature generation because of the excessive frictional pressure at the tool-chip interface leads to thermal distortions to the workpiece in addition to tool material [14]. Performance characteristics like tool flank wear, attentive surface roughness and chip morphology analysis of has been examined using bearing steel [15]. Accelerated spray cooling environment has been introduced that leads to improving the heat transfer as well as reduction of friction during machining of hard D2 steel [15].

Nowadays, implementation of nanofluid minimum quantity lubrication (NFMQL) is more demanding because of its better tribological and thermo-physical characteristics which provide improved output characteristics such as surface finish and lower tooling wear compared with the other lubrication strategies [16]. The adding of nanoparticles in the base fluids has improved thermal conductivity remarkably [17]. The thermal conductivity of the nanofluids rises by the augment of particle wt% of nanoparticles in the base fluid [18]. SiO<sub>2</sub> nanoparticles, when used as a lubricant produce a preservative film (thin) on the machined surface wherein rolling motion of billions of nanoparticles on the chip-tool boundary reduces the coefficient of friction eventually lowering the force experienced by the cutting tool and thus accounts for the minimization of cutting temperature, tool wear and holds good for the better surface finish. Adding up of nanometre-sized solid particles to the traditional cutting fluid can advance thermo-physical characteristics. These fluids include nanoparticles, termed as “nanofluids” having benefits, for example, better thermal conductivity and stability, and lubricating characteristic compared to the base fluid. Aluminum oxide nanofluid reveals lower viscosity and high thermal conductivity and compared to Titanium Oxide and Silicon Oxide nanofluids [19].

Four distinguish types of deionized water-based nanofluids (Al<sub>2</sub>O<sub>3</sub>, ZnO, CuO, and Fe<sub>2</sub>O<sub>3</sub>) were utilized in hard turning of AISI 4340 grade steel. Among these nanofluids, CuO was performed superior succeeded by ZnO, Fe<sub>2</sub>O<sub>3</sub> and Al<sub>2</sub>O<sub>3</sub> [20]. Rice bran vegetable oil-based MQL assisted three different nanofluids namely CuO, Fe<sub>2</sub>O<sub>3</sub> and Al<sub>2</sub>O<sub>3</sub> were utilized in the machining of 4340 alloys (47 ± 1 HRC) steel. Among these nanofluids, CuO attributed the best performance followed by Fe<sub>2</sub>O<sub>3</sub> and Al<sub>2</sub>O<sub>3</sub> [21]. Three different cooling mediums like compressed air, water-soluble oil and MQL applied Al<sub>2</sub>O<sub>3</sub> nanofluid were applied to study the diverse machining responses in hard turning of heat-treated 4340 steel. Al<sub>2</sub>O<sub>3</sub> nanofluid outperformed relatively other cooling mediums [22]. Tool life comparison was studied in hard turning of heat-treated D2 tool steel under normal water and TiO<sub>2</sub> nanofluid surroundings using spray impingement technique. Nanofluid enriched coolant attributed a 70 % gain in tool life compared to normal water [23]. Water can be used as a coolant because of its copiousness; low-price and better thermal conductivity However, because of its corrosive nature, appalling lubricating potential limited its implementations in contemporary days of machining. The researchers located that water-oil emulsion reveals advanced cooling and lubrication distinctiveness and this is caused by the delivery of an advance magnificence of machining fluid-based totally on mineral and vegetable oils [24]. Dry cutting and mist cooling assisted hard turning on EN 24 (48 HRC) steel were performed and compared. Chip micro-hardness and cutting force are favorable under dry cutting while crater and flank wear, surface quality and chip morphology were advantageous under water-soluble oil assisted mist cooling [25]. Sopian et al. utilized pulse jet MQL

in slot milling operation and found advantageous results of tool wear and surface roughness compared to dry and flood cooling assisted milling [26].

The cutting tool wear is reduced in the machining of hard to cut materials like Incoloy at higher cutting speeds and feeds with a cemented carbide tool. Due to the reduced cutting attributes of the uncoated cemented carbide, tooling life is shortened and proper surface finish may not be accepted in many circumstances. Consequently, the cutting traits may be advanced by using two distinguish coating techniques namely Physical Vapor Deposition (PVD) and Chemical Vapor Deposition (CVD). Further, PVD based tool cover more than a few families of vacuum operation wherein the coating material is physically eliminated from a supply through evaporation [27]. TiAlN coated tool experienced minimum flank wear and also decrease in cutting force components which raised the tooling life and also helped in achieving better surface finish by increasing the chip fragility [28]. TiAlN PVD coated cutting tool encounters lower cutting force and with its lubrication capabilities, higher Vickers hardness number and anti-adhesion characteristics justify its use in the machining of hard to cut material to achieve better tooling life and surface quality [29].

Though lots of research work has been focused on experimental analysis and its output characteristics of hard to cut materials, there is no research has been focused on machinability study on turning of Incoloy 330 using nanofluid. Also, only a few researchers have focused on the selection of optimum concentrations of nanoparticles that can be used in cutting fluid to achieve a better cutting performance in the turning process for hard to cut materials. Further, coconut oil-based nanofluid is rarely used in any machining application. However, considering these research gaps, the present work presents a systematic evaluation of the effects of MQL using Nanofluids on machining difficult to cut material like Incoloy 330. Nanoparticles  $\text{SiO}_2$  is mixed with coconut oil as the base fluid. Herein, three different concentrations of 0.1 %, 0.2 % and 0.3 % of  $\text{SiO}_2$  nanofluids are prepared and used through MQL as a lubricating agent while machining Incoloy 330 with a TiAlN coated PVD cutting tool.

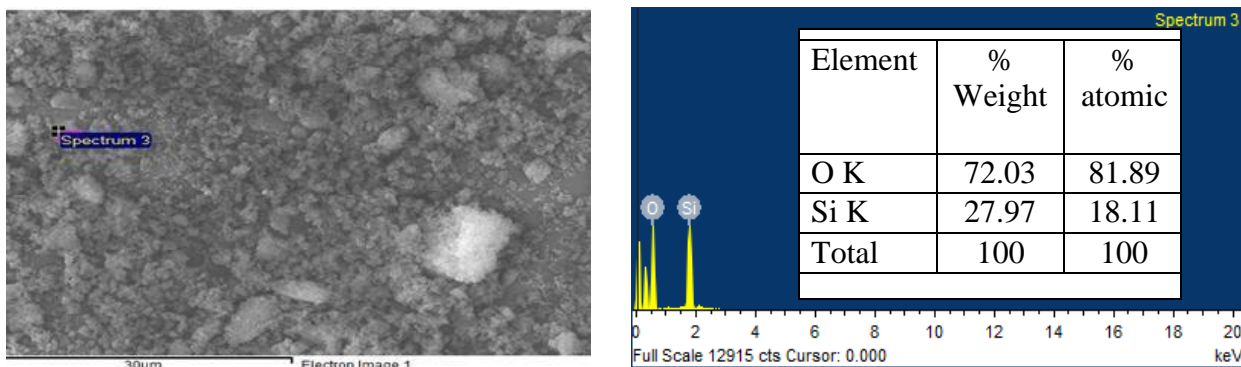


Fig 1 - EDS analysis of  $\text{SiO}_2$  nanoparticles

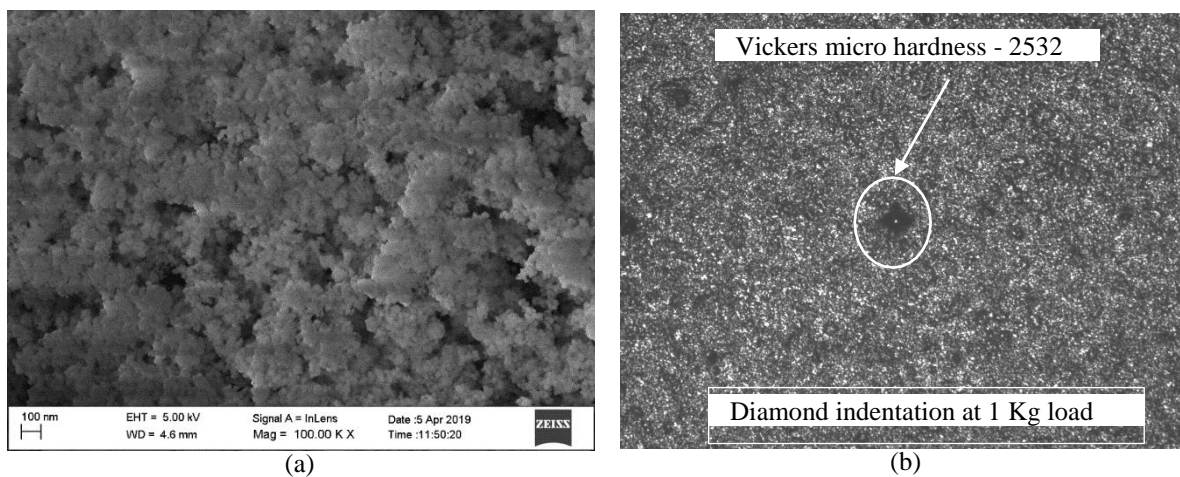


Fig. 2 - (a) SEM image of  $\text{SiO}_2$  nano particle (b) Vickers micro hardness of cutting insert

## 2. Experimental methodologies

The turning experiments are performed in the MQL environment using three different concentrations of coconut oil-based  $\text{SiO}_2$  nanofluids with three different weight % concentrations (0.1, 0.2, and 0.3). The nanoparticle is supplied by Sisco Research Laboratories Pvt. Ltd. India and the particle size is varied from 15-25 nm. The elemental

composition of nanoparticles has been verified using Energy Dispersive Spectroscopy (EDS) analysis as shown in Fig 1, which confirms the presence of associated elements in SiO<sub>2</sub> nanopowders. Particle size measurement has been carried by Scanning Electron Microscope (SEM) image as displayed in Fig 2a. The size of the particles is found to be in the range of 15-25 nm (average size 20 nm). In the literature, the size of the SiO<sub>2</sub> nanoparticles mostly found to be less than 50 nm [19, 29].

The fluid is prepared by pouring the nanoparticles (SiO<sub>2</sub>) in the base fluid (Coconut oil) and is mixed with the help of a magnetic stirrer for two hours. Next, to obtain a proper consistent and steady suspension, the nanofluids are then kept in the sonicator bath for 1 hour. The sonicator generates ultrasonic pulses of 100 W at 36± kHz. CNC lathe machine is used for the turning operation. Incoloy 330 alloy of 57 mm diameter and 220 mm length is selected as a test sample for the experimentation. In general, Incoloy 330 has nickel content of 34% to 37% and chromium content of between 17% to 20% and it is incredibly resistant to oxidation at high temperatures up to 1148°C. The elemental composition in % weight of selected Incoloy 330 is as follows: Fe-43.83, Ni-34.80, Cr-8.24, Mn-1.32, Si- 1.125, C-0.08, S-0.030 and P-0.030. The mechanical properties of Incoloy 330 are presented in Table 1. PVD Coated TiAlN cemented carbide tool (CNMG 120408) with an a 95° approach angle, negative rake angle of -6° and nose radius of 0.8 mm, commercially available supplied by WIDIA is used for machining in this present work. The cutting inserts were attached rigidly into a tool holder of PCLNR 2525 M12 ISO designation. The micro hardness test of TiAlN coated cemented carbide insert was carried out by the Vickers micro-hardness tester using 1 Kg load and the micro-hardness (HV) is found to be 2532 as displayed in Fig 2b. To perform the experimental work, L<sub>9</sub> Taguchi orthogonal array has been used as the Design of Experiment (DOE). The experiments have been carried out with constant depth of cut of 0.2 mm, MQL flow rate is 20 (ml/h) and three variable input parameters like concentration of nanofluids (Nc), feed (f) and cutting speed (Vc) are chosen. The process parameters and their levels are presented in Table 2. The focal aim of the current research is to investigate the flank wear (VBc), surface roughness (Ra), material removal rate (MRR), and Chip morphology under MQL assisted machining. Taylor-Hobson (Surtronic 25) surface roughness tester is utilized to assess the surface roughness of the finished machined part and it was calibrated using a standard specimen before it was used for measuring the average arithmetic surface roughness. Chip images and flank wear images were taken by Olympus STM6 Optical Microscope (Made in Japan). The schematic outline of experimental work is reported in Fig 3.

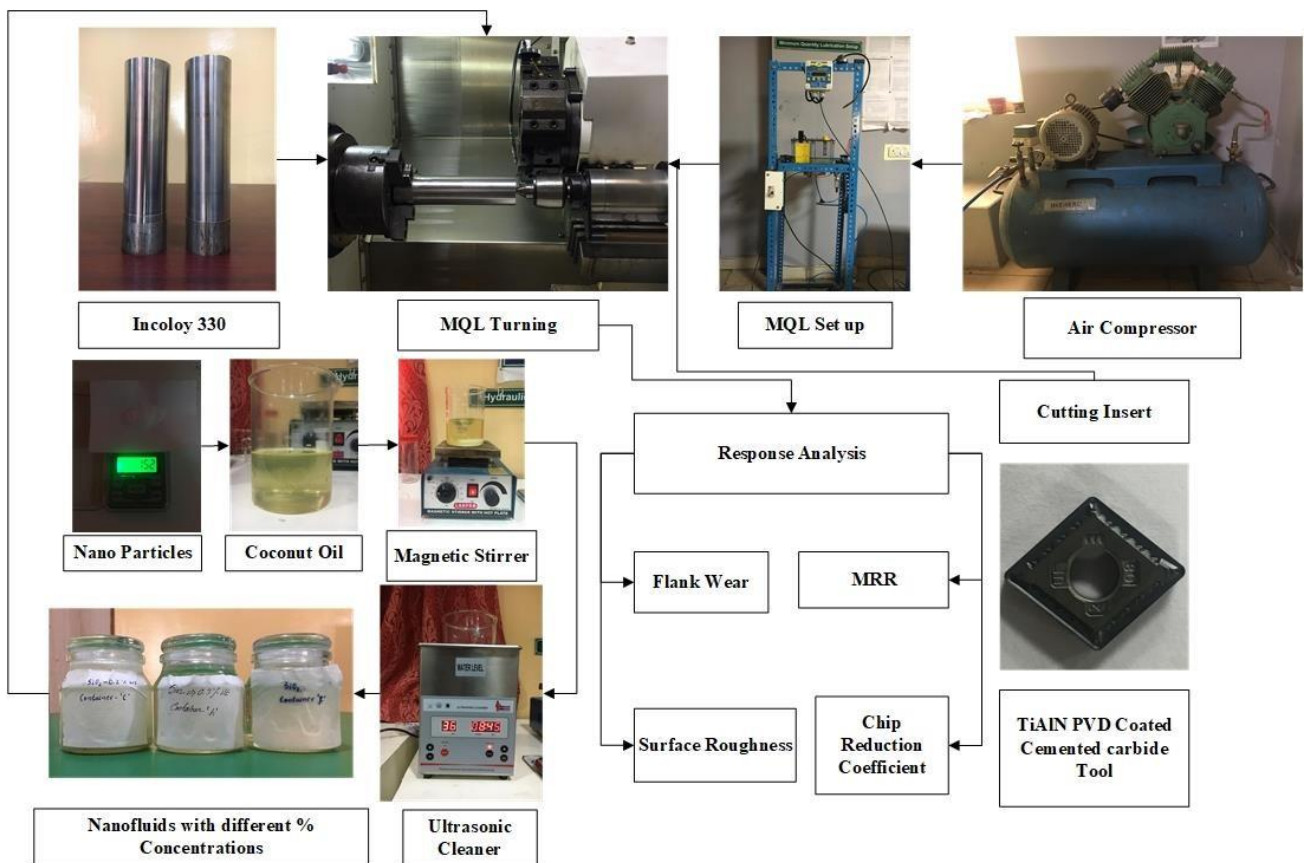


Fig. 3 - Schematic outline of experimental setup

**Table 1- Mechanical Properties of Incoloy 330**

Properties	Value
Tensile Strength (MPa)	600
Yield Strength (MPa)	280
Poisson's ratio	0.340
Specific Heat (J/kg. °C)	460
Density (gm/cm <sup>3</sup> )	8.08
Melting Range (°C)	1380-1420

**Table 2 - Process parameters**

Input terms	Symbols	Units	Levels of inputs		
			I	II	III
Concentrations	Nc	% weight	0.1	0.2	0.3
feed	f	mm/rev	0.15	0.25	0.35
Cutting speed	Vc	m/min	80	120	160

### 3. Result and discussions

The Incoloy 330 bar has been turned using PVD coated insert using the L<sub>9</sub> set of experiments and the input as well as experimental results of all responses is reported in Table 3.

**Table 3 - L<sub>9</sub> design and the experimental results**

Test No.	L <sub>9</sub> input parameters			Experimental results		
	Nc (% weight)	f (mm/rev)	Vc (m/min)	VBc (mm)	Ra (µm)	MMR (g/sec)
1	0.1	0.15	80	0.057	0.94	0.000275
2	0.1	0.25	120	0.065	1.51	0.000825
3	0.1	0.35	160	0.077	1.89	0.001602
4	0.2	0.15	120	0.063	1.04	0.000542
5	0.2	0.25	160	0.074	1.53	0.001246
6	0.2	0.35	80	0.064	1.67	0.001016
7	0.3	0.15	160	0.071	1.11	0.00089
8	0.3	0.25	80	0.061	1.28	0.000592
9	0.3	0.35	120	0.068	1.72	0.001378

#### 3.1 Tool-flank Wear Analysis

In machining, the forever aim of the manufacturers is to reduce the machining cost by minimizing the tool wear rate. Currently, tool-flank wear analysis of the TiAlN PVD coated carbide tool in the machining of Incoloy 330 has been conducted based on microscopic images of tool-tip wear (Fig. 4). The results (Table 3) revealed that the cutting tool experienced minimum ranges of flank wear as wear width varies from 0.057 to 0.077 mm due to excellent lubrication and cooling capabilities of coconut oil-based SiO<sub>2</sub> nanofluid. During machining under nanofluid, a thin protective film on tool tip-work interface generated which helps in reducing the friction thus cutting zone temperature as well as flank wear reduces [19]. Also, high Vickers hardness number of insert justify its use in machining hard to cut material Incoloy 330 to achieve a lower wear rate and better tool life [29]. From the Table 3, the higher wear width occurred at higher cutter speed and feed condition, i.e. wear width gradually increases with cutting speed and feed. From the optical image of worn tool-tip, the major wear mechanisms of the tool are noticed as built-up edge (BUE) formation, abrasion, adhesion, micro-chipping (small amount of tool material removed from the edge of tool-tip) and chipping. Among all, BUE and abrasion are dominating in nature as in the majority of cases these mechanisms are noticed on tool-tip [30]. In most experiments, BUE develops during moderate or high-speed machining due to high-temperature generation during machining which formed a welded like structure as some portion of chips gets adhered to the tool-tip. According to Akhtar et al. [31], BUE is a kind of protective layer over the tool-tip and it is very unstable during cutting. Therefore, sometimes, it gets broken and separated from tool-tip with carrying some tool materials. These phenomena cause micro-chipping as well as chipping of the tool-tip. This chipping off affects the geometry of the tool and may accelerate the tool premature failure and poor surface finish of the machined portion. Abrasion phenomena is a common wear mechanism noticed during machining of nickel-based alloys [30, 32]. It occurs due to flowing coiled helical chips which have hard particles like nickel (Ni) and chromium (Cr) and it is continuously rubbed with the tool- tip-flank surface, as a result, it erodes the flank surface of tool-tip and shine marks are observed on the flank face of the tool as shown in Fig. 4.

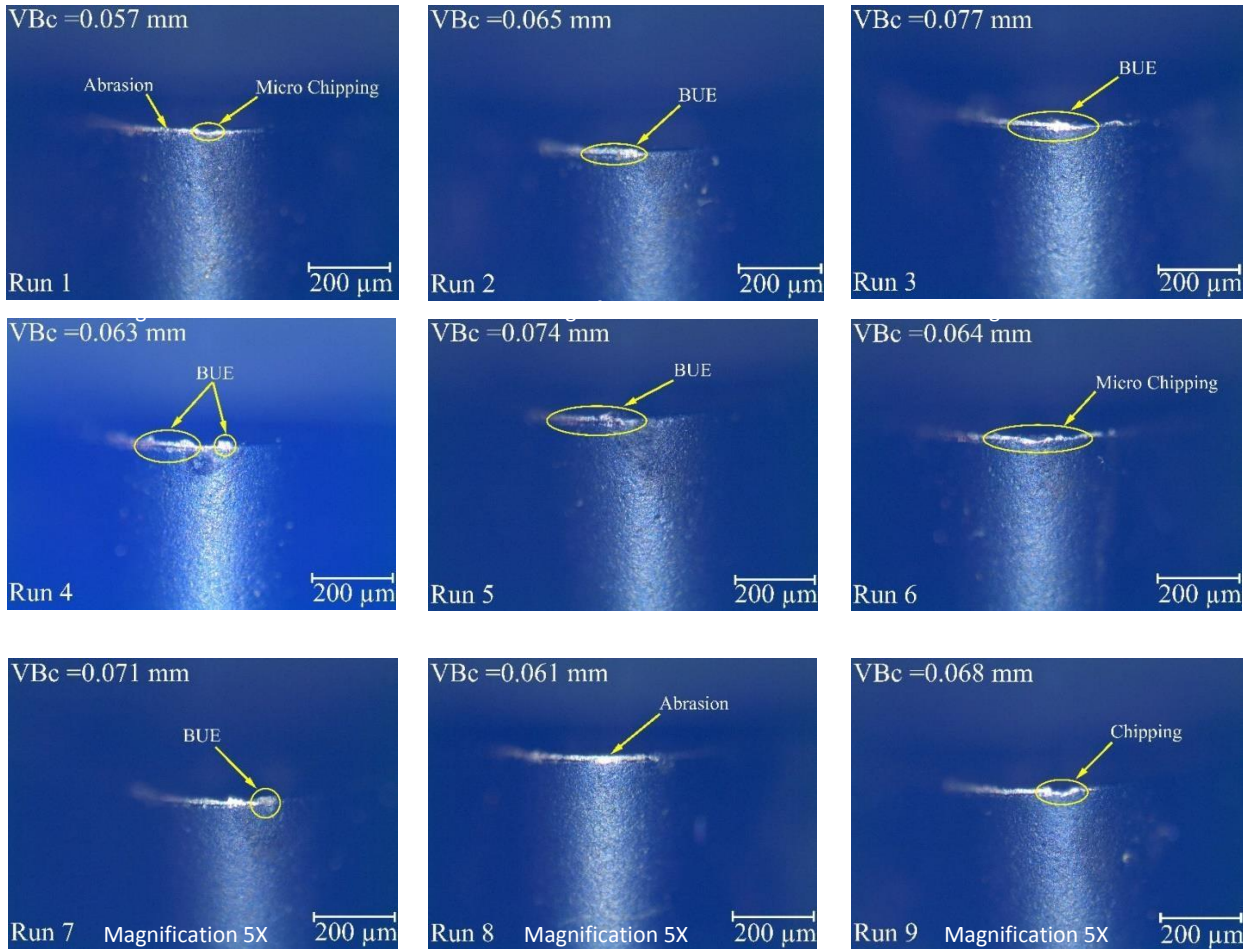


**Fig. 4 - Optical image of tool-flank wears**

3D surface plots (Figs. 5a-b) indicates that the flank wear is strongly affected by the cutting speed as surface slope elevating sharply with the increase in cutting speed ( $V_c$ ) from 80 to 160 m/min. Similarly from Figs. 5b-c, feed ( $f$ ) also effectively influences the flank wear as surface is gradually elevating with an increase in the feed from 0.15 to 0.35 mm/rev [33]. The influence of nanoparticle concentrations ( $N_c$ ) on tool wear is negligible as the surface slope in Fig. 5a and Fig. 5c is uneven. It indicates that the variations considered in nanofluid concentrations are not much effective, therefore it is recommended to take higher nanoparticle concentrations of  $SiO_2$  to investigate the machinability characteristics of Incoloy 330. From the surface plot (Fig. 7), it can be stated that the combined effect of each pair terms like  $Nc1-Vc3$ ,  $Vc3-f3$  and  $Nc1-f3$  attributed the highest peak corner of  $VB_c$  which confirms the highest flank wear generation during machining. ANOVA (Table 4) also confirmed that the cutting speed is the strongest term which influences the wear highest as its contribution is highest (83.24%) among all input terms while feed contributing the wear next to feed with 16.36% of contribution [15, 34]. A negligible contribution (0.2%) of the nanoparticle is found on tool wear.

**Table 4 - ANOVA findings for  $VB_c$**

Terms	DF	Seq SS	Adj MS	F	P	Contribution (%)	Interpretations
$N_c$	2	0.0000007	0.0000002	1.00	0.500	0.212	Insignificant
$f$	2	0.0000540	0.0000270	81.00	0.012	16.36	Significant
$V_c$	2	0.0002747	0.0001373	412.00	0.002	83.24	Significant
Error	2	0.0000007	0.0000003				
Total	8	0.0003300					

$S = 0.000577350$      $R-Sq = 99.80\%$      $R-Sq(adj) = 99.19\%$

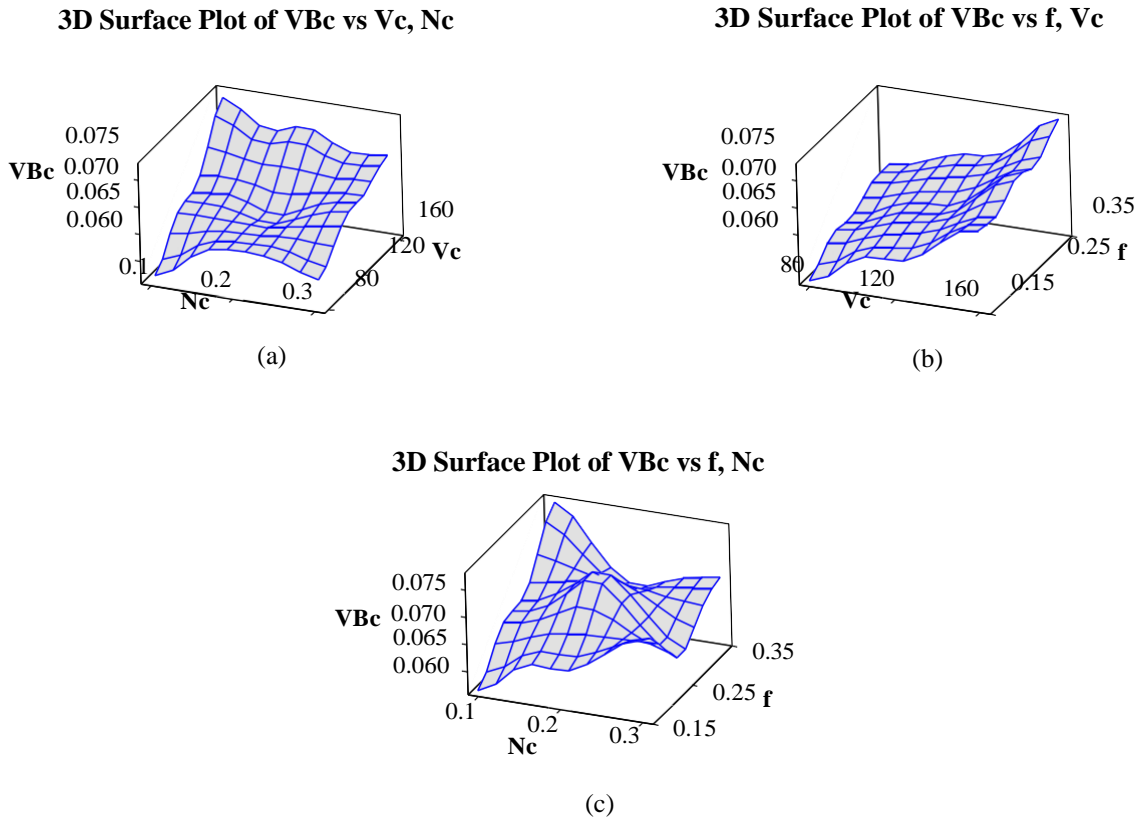


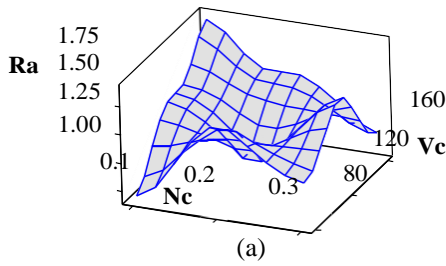
Fig. 5 - 3D surface plot for VBc

### 3.2 Machined surface roughness analysis

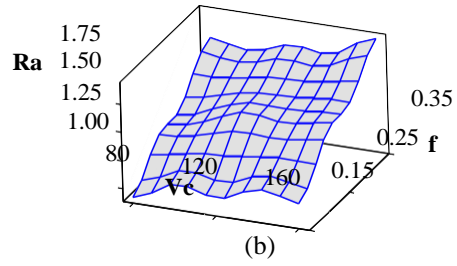
The principal target of any manufacturing industries is to achieve a better surface finish of the machined part in a productive way. Since a few years, researchers are trying hard to achieve a better surface roughness with low production cost. From the test results (Table 3), surface roughness (Ra) is leading with feed rate and cutting speed while reduces with increasing nanofluid concentrations due to development of a thin preservative film in between tool- work surface and also, rolling motion of nanoparticles on the tool-chip interface reduces the coefficient of friction between tool-chip-workpiece, thus reduction in machining temperature and tool wear takes place which attributed the better surface finish [15]. Machining on the highest feed value (0.35 mm/rev) attributed the higher range of Ra (above than a favorable limit of 1.6  $\mu\text{m}$ ) [35]. It may occur due to poor penetration of nanofluid into the cutting zone. At the highest feed tool movement is very fast, therefore there is a lack of time to penetration nanofluid through capillary action into cutting zone thus insufficient lubrication between tool-chip-workpiece took place. Also, from literature, it was found that the surface roughness was increasing with feed value and the highest Ra was achieved at the highest feed value [34, 36].

Further, effects of cutting terms on Ra are studied through 3D surface plots (Fig. 6) and found that the surface roughness is principally influenced by feed rate as the surface slope is almost uniformly elevating with the rise in feed value. Further, Ra is also significantly influenced by cutting speed (Vc), as the surface graph is sharply increasing with increasing cutting speed as indicated in Fig. 6a. The effect of Nc on Ra is least as surface slope variation is uneven. Also, from Fig. 6, the highest peak corner of the surface plot is found at the combination of each Nc1-Vc3 (Fig. 6a), Vc3-f3 (Fig. 6b) and Nc1-f3 (Fig. 6c) pair, which shows the worst quality of finish at these combinations of input terms. Similarly, a lowest corner of the surface plot is found at the combinations of terms Nc1-Vc1 (Fig. 6a), Vc1-f1 (Fig. 6b) and Nc1-f1 (Fig. 6c), i.e. best quality of finish are achieved at these input combinations. However, for surface finish concern, a combination of the lowest level of each input term is recommended for turning [35-36]. ANOVA (Table 5) also confirms the dominance of feed on Ra with the highest contribution of 90.96%. The next dominant term for Ra is cutting speed with 7.82% contribution while nanofluid concentration is not contributing any relevant effect on Ra as their p-value is 0.174 which is higher than 0.05 at 95 % of confidence level [15, 34, 37].

**3D Surface Plot of Ra vs Vc, Nc**



**3D Surface Plot of Ra vs f, Vc**



**3D Surface Plot of Ra vs f, Nc**

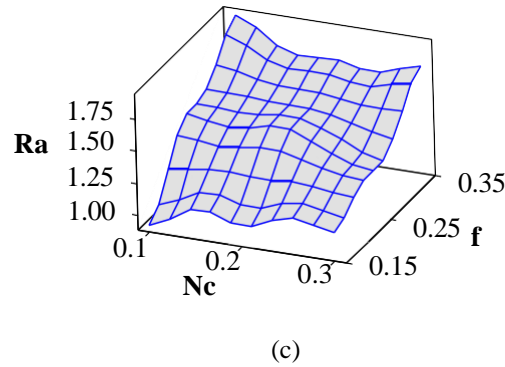


**Fig. 6 - 3D Surface plot of Ra**

**Table 5 - ANOVA findings for Ra**

Terms	DF	Seq SS	Adj MS	F	P	Contribution (%)	Interpretations
Nc	2	0.00887	0.00443	4.75	0.174	1.00	Insignificant
f	2	0.80340	0.40170	430.39	0.002	90.96	Significant
Vc	2	0.06907	0.03453	37.00	0.026	7.82	Significant
Error	2	0.00187	0.00093				
Total	8	0.88320					

S = 0.0305505    R-Sq = 99.79%    R-Sq(adj) = 99.15%

### 3.3 Material Removal Rate Analysis

Rate of the material removal is very essential in machining as a higher MRR rate reduces the machining time and thus the production costs. From the test results (Table 3), it is seen that with an increase in cutting speed and feed rate MRR increases but on the other hand surface quality deteriorates. Marimuthu et al. [38] found that the MRR was highly influenced by feed and depth of cut during machining of Inconel 625 using TiAlN coated carbide insert. The highest MRR (0.001602 g/sec) is obtained at highest feed rate (0.35 mm/rev) and at highest cutting speed (160 m/min) whereas; lowest MRR (0.000275 g/sec) is obtained at lowest cutting speed (80 m/min) and lowest feed rate (0.15 mm/rev) condition. From the test result, run no 5 is most suitable to achieve higher MRR, acceptable surface quality (< 1.6µm) and acceptable wear width (< 0.3 mm).

From the 3D surface plot of MRR (Fig.7), it is observed that feed and cutting speed strongly affect the values of MRR. Combine effects of Nc and Vc are presented in Fig. 7a, and it can be visualized that the lowest parametric value of Nc (0.1 wt%) with a combination of the highest value of Vc (160 m/min) attributed the highest MRR. Further the combined effect of f-Vc greatly influences the MRR as the surface slope is elevating with increment in feed and Vc and the highest MRR is achieved at a higher level of these parameters. Similarly, lowest Nc (0.1 wt%) with combination of highest feed (0.35 mm/rev) exhibited the highest MRR. However, it can be summarized that the combination of lowest

Nc (0.1 wt%) with the highest feed (0.35 mm/rev) and cutting speed (160 m/min) attributed the highest MRR. ANOVA (Table 6) confirmed that the cutting feed is the most dominating term for MRR with a 60 % contribution followed by cutting speed with a 40 % contribution while there is no effect of nanofluid on MRR.

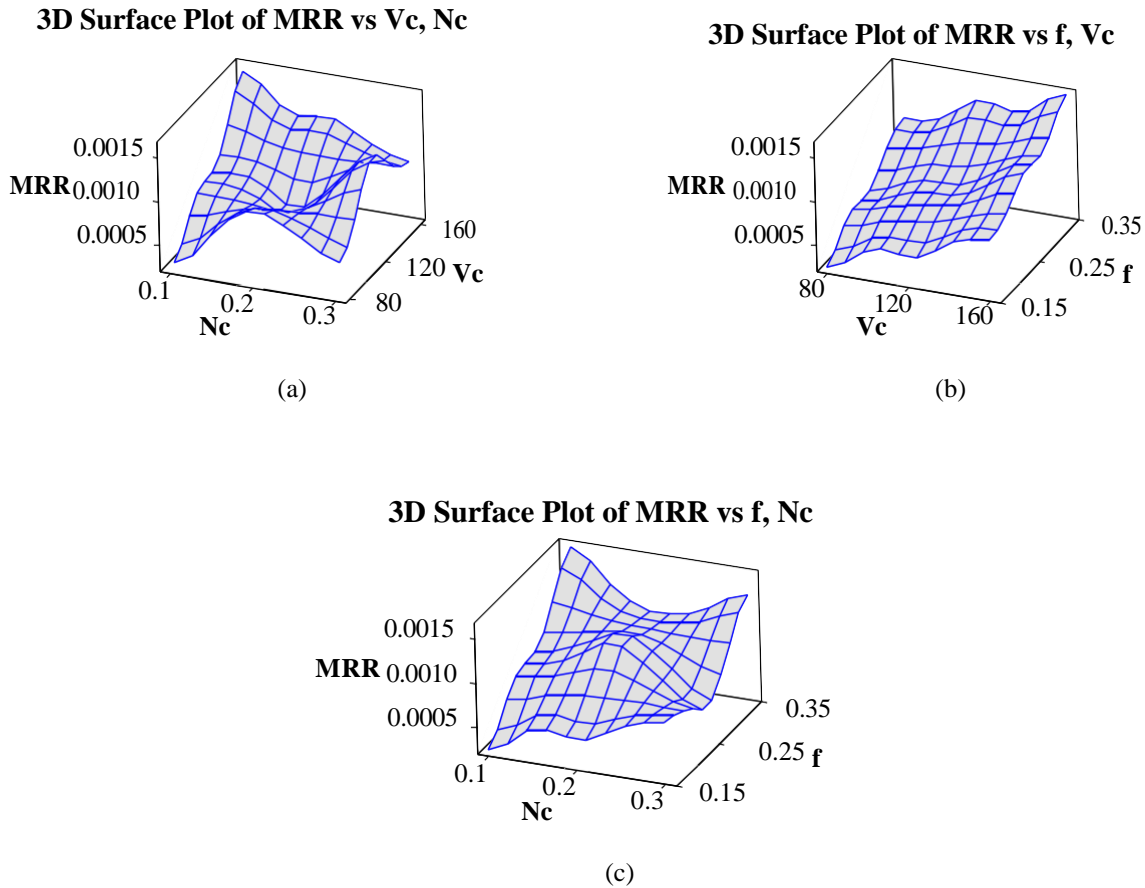


Fig. 7 - 3D surface plots of MRR

Table 6 - ANOVA findings for MRR

Terms	DF	Seq SS	Adj MS	F	P	Contribution (%)	Interpretations
Nc	2	0.0000000	0.0000000	0.70	0.587	0.00	Insignificant
f	2	0.0000009	0.0000004	144.67	0.007	60.00	Significant
Vc	2	0.0000006	0.0000003	94.31	0.010	40.00	Significant
Error	2	0.0000000	0.0000000				
Total	8	0.0000015					

S = 0.0000551855 R-Sq = 99.58% R-Sq(adj) = 98.34%

### 3.4 Chip morphology

In the turning process, the maximum amount of heat is carried away from the cutting zone by the chip formed. So, studying the chip morphology becomes very crucial in analyzing the tool-chip interface correlation to figure out the appropriate cutting parameters under nanofluid-MQL environment. In entire experimental tests, coiled continuous helical chips are obtained. The colour of chips is found to be metallic only which signifies that the cutting temperature evolved is less and better for machinability aspects. Angappan et al. [39] found long helical, coiled helical and ribbon type of chips in dry cutting of Incoloy 800H. Chip serration is clearly visible on the bottom face of chips and further deformation leads to side flow of material at edges of chips. Similar observations have been made by Thakur et al. [40] in the dry machining of Incoloy 825. The chip curl angle ( $\theta$ ) is measured using stream basic software and it is the angle between tangents of chip edge as shown in Fig. 8. Measured chip curl angle (Fig. 8 and Table 7) reduces with cutting

speed due to minimal time existing for the chip to curl owing to the impingement of nanofluid. According to Bhatt et al. [41], the phenomena of chip curling are highly depending on temperature gradient (temperature difference in between the free or top surface and sliding surface). However, in the current context nanofluid through MQL is impinged on to the free surface so temperature reduces but the sliding surface has more temperature due to friction so temperature gradient exists so chip curling takes place. From (Fig. 9a), the chip curl angle is also increased with nanofluid concentration due to the increasing thickness of the hydrodynamic layer between chip and tool top face [32]. Chip curl angle also increases with feed till 0.25 mm/rev but beyond this, it reduces. Higher chip curl diameter was found in the cutting process due to may larger contact friction between sliding surfaces during turning operations [39].

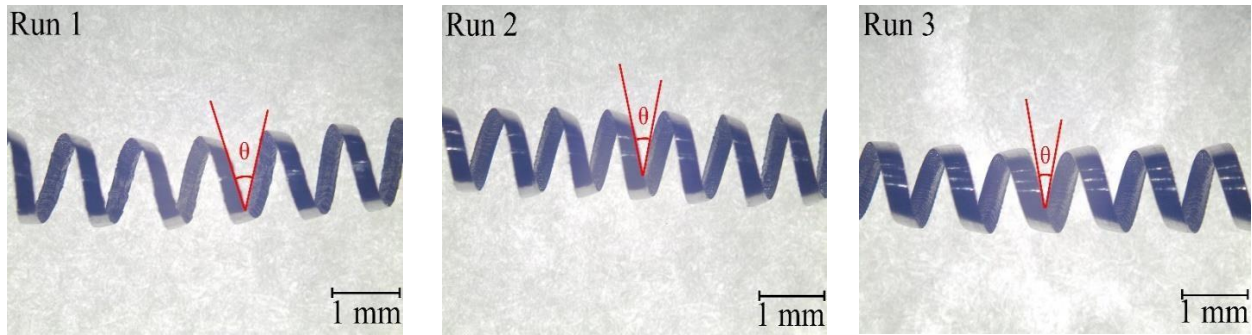


**Fig. 8 - Optical micrographs of formed chips**

The measurement of chip reduction coefficient ( $\zeta$ ) is an essential machinability index, as it shows machining behavior like favorable or unfavorable machining in terms of specific consumption. It is the extent of plastic deformation in cutting action [30, 34]. A low magnitude of chip reduction coefficient indicates a smaller shear angle and lower extent of plastic deformation and thus lower specific energy consumption. Analytically, the chip reduction coefficient is the ratio of the measured deformed thickness of chip ( $a_2$ ) to the un-deformed chip thickness ( $a_1$ ) [15, 30, 34]. Uncut chip thickness ( $a_1$ ) is the product of feed rate and  $\text{Sin } \phi$  where ‘ $\phi$ ’ represents the approach angle. The value of un-deformed chip thickness ( $a_1$ ), deformed chip thickness ( $a_2$ ) and chip reduction coefficient ( $\zeta$ ) are reported in **Table 7**. Deformed chip thickness varies between 0.3 to 0.74 mm which is found to be low due to the application of nanofluid through MQL which enhanced the heat dissipation thus eliminated the tendency of chip welding on the top surface of the tool [32]. Further, from (**Fig. 9b**), deformed chip thickness increases with feed rate which is similar to work carried by [32]. Also, chip thickness reduces with cutting speed while the effects of nanofluid concentrations are negligible. Thakur et al. [40] and Talib et al. [42] also stated that the chip thickness was reducing with increasing cutting speed due to enhancement in material removal per revolution and reduction in chip-tool sliding friction. In machining, lower chip thickness attributes to the smaller shear plane with a bigger shear angle as a result friction coefficient reduces thus cutting forces reduces and similar studies were reported in previous works [30]. From (**Fig. 9c**), the chip reduction coefficient is getting down with improving feed and cutting speed while the effects of nanofluid concentration are negligible [15, 34].

**Table 7 - Measured value of chip curl angle, chip thickness and chip reduction coefficient**

Sr. No.	$N_c$ (% Wt)	$f$ (mm/rev)	$V_c$ (m/min)	$\theta$ (Degree)	$a_1 = f \cdot \text{Sin } 95$ (mm)	$a_2$ (mm)	$\zeta = a_2/a_1$
1	0.1	0.15	80	31.38	0.102	0.36	3.529
2	0.1	0.25	120	30.13	0.170	0.49	2.882
3	0.1	0.35	160	28.88	0.239	0.57	2.385
4	0.2	0.15	120	29.96	0.102	0.33	3.235
5	0.2	0.25	160	29.67	0.170	0.45	2.647
6	0.2	0.35	80	31.90	0.239	0.74	3.096
7	0.3	0.15	160	26.48	0.102	0.3	2.941
8	0.3	0.25	80	36.44	0.170	0.58	3.412
9	0.3	0.35	120	30.88	0.239	0.65	2.720

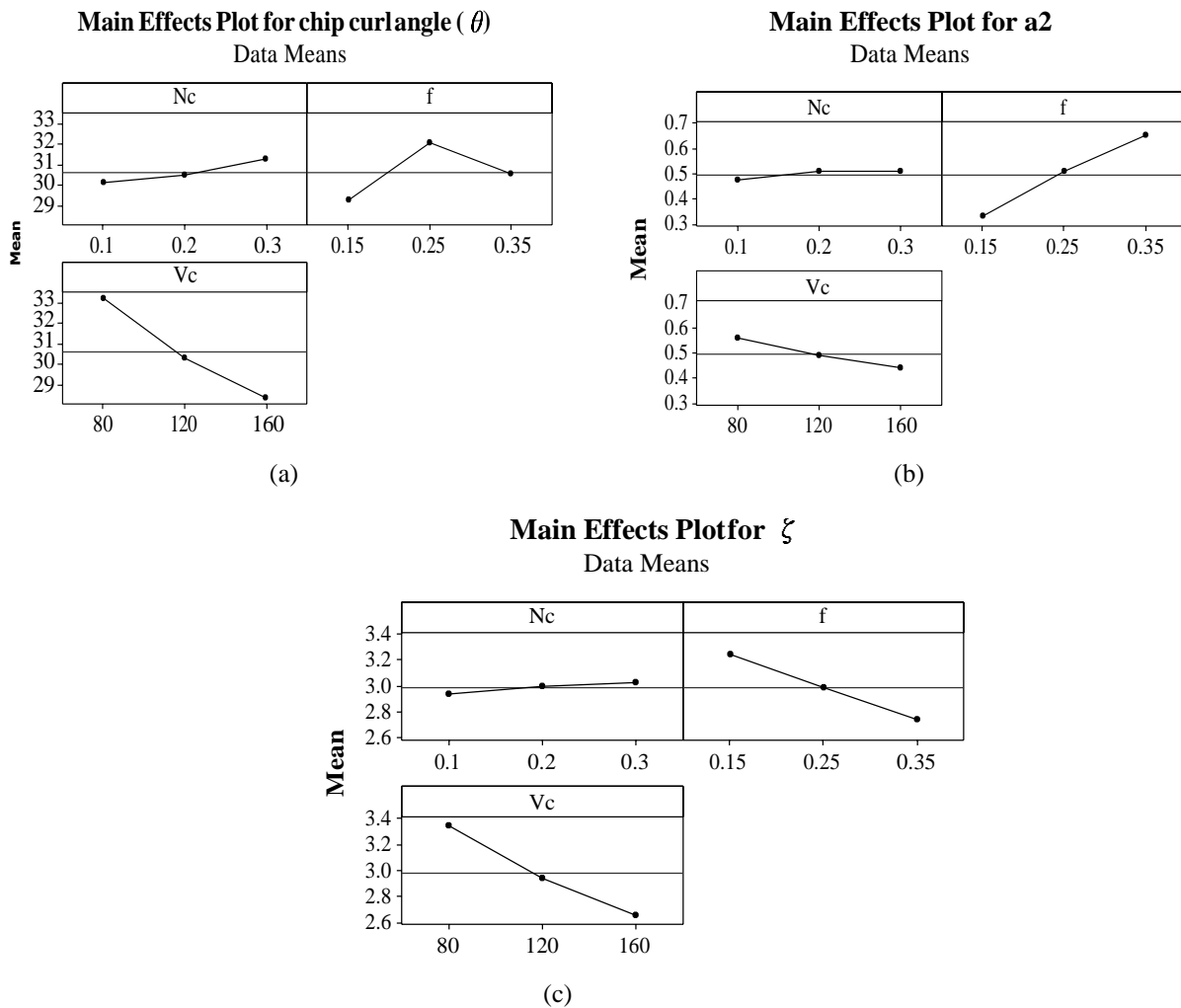


**Fig. 9 - Effects of input terms on (a) chip curl angle; (b) chip thickness; (c) chip reduction coefficient**

#### 4. TOPSIS multi response optimization

Herein, TOPSIS (Technique for Order of Preference by Similarity to Ideal Solution) optimization technique has been utilized for the parametric optimization of the multi responses (VBc, Ra, and MRR) using the steps mentioned in Eqs. 1-4 [43-46]. TOPSIS is used for selecting the best alternative based on the criteria that the substitute chosen must have the smallest gap from the beneficial criteria and the farthest distance from the non-beneficial criteria. Here, beneficial criteria are the ones that improves on the efficiency standards and minimize the unfavorable standards, and non-beneficial criteria are the ones that minimizes the efficiency standards and maximizes the unfavorable standards [45]. Responses data are normalized using the first step and reported in Table 8. Further in the second step, using equal weight criteria i.e. Weight of VBc = Weight of Ra = Weight of MRR = 0.33, the weighted normalized matrix is estimated and presented in Table 9. Further, the best positive and worst negative values are estimated with help of third step and reported in Table 10. Next, using the fourth step, the ideal best and ideal worst value is calculated and reported in Table 11. Further, using the fifth step, the closeness coefficient (Pi) is reported in Table 11. Moreover, the mean performance coefficient is estimated as shown in Table 12. Higher the mean value of individual input terms confirms their respective levels. Therefore from Table 12, the optimum set of parameters are found to be 3<sup>rd</sup> level of nanofluid concentration (Nc) = 0.3 % wt, 1<sup>st</sup> level of feed (f) = 0.15 mm/rev and 3<sup>rd</sup> level of cutting speed (Vc) = 160 m/min. Using the optimal set of parameters, a confirmatory test is carried and found to be 0.1692 or 44% gain in the performance coefficient (Pi) from the initial setting. Thus, the used TOPSIS method is efficient to optimize the response data for engineering problems.

Step 1: - The normalized decision matrix is computed using the Eq.1.

$$V_x = \frac{N_{ij}}{\sqrt{\sum_{i=1}^n N_{ij}}} \tag{1}$$

Where  $i = 1, 2, \dots, n$ ;  $j=1, 2, \dots, m$ ,  $N_{ij}$  is the actual value of the  $i^{\text{th}}$  value of  $j^{\text{th}}$  trial run and  $V_x$  is the normalized value.

Step 2: The normalized value matrix is converted into a weighted value matrix by multiplying with reciprocal of the weighted criteria i.e.;  $(1/3=0.33)$

Step 3: Further, the best positive value ( $V^+$ ) and a worst negative value ( $V^-$ ) is calculated by choosing the appropriate value against the respective criteria. For beneficial criteria like MRR highest value is required in  $V^+$  and the lowest value is required in  $V_j^-$ . On the other hand, for the non-beneficial criteria like VBc, and Ra, the lowest value is required in  $V_{j^+}$  and the highest value is required in  $V_{j^-}$ .

Step 4: Estimate the Euclidean distance  $Si^+$  and  $Si^-$  from the ideal best and ideal worst values as noted in Eq. (2) to (3):

(3)(3):

$$Si^+ = \left[ \sum_{j=1}^r (V_{ij} - V_j^+)^2 \right]^{0.5} \tag{2}$$

$$si^- = \left[ \sum_{j=1}^r (V_{ij} - V_j^-)^2 \right]^{0.5} \tag{3}$$

Step 5: The closeness coefficient (Pi) is calculated by the following Eq. 4.

$$P_i = (s_i^- / s_i^- + s_i^+) \tag{4}$$

**Table 8 - Normalization matrix**

Test No.	VBc	Ra	MRR
1	0.2838	0.2169	0.0905
2	0.3237	0.3485	0.2714
3	0.3834	0.4362	0.5269
4	0.3137	0.2400	0.1783
5	0.3685	0.3531	0.4098
6	0.3187	0.3854	0.3342
7	0.3535	0.2562	0.2927
8	0.3037	0.2954	0.1947
9	0.3386	0.3969	0.4533

**Table 9 - Weighted normalized matrix**

Test No.	VBc	Ra	MRR
1	0.0937	0.0716	0.0299
2	0.1068	0.1150	0.0543
3	0.1265	0.1439	0.1054
4	0.1035	0.0792	0.0357
5	0.1216	0.1165	0.0820
6	0.1052	0.1272	0.0668
7	0.1167	0.0845	0.0585
8	0.1002	0.0975	0.0389
9	0.1117	0.1310	0.0907

**Table 10 - Best positive and worst negative value**

	<b>VBc</b>	<b>Ra</b>	<b>MRR</b>
$v_j^+$	0.0937	0.0716	0.1054
$V_j^-$	0.1265	0.1439	0.0299

**Table 11-Performance coefficient (Pi) and their ranks**

<b>Test No.</b>	$S_i^+$	$S_i^-$	$P_i$	<b>Rank</b>
1	0.0755	0.0795	0.5127	2
2	0.0683	0.0427	0.3845	9
3	0.0795	0.0755	0.4873	6
4	0.0708	0.0689	0.4932	5
5	0.0579	0.0591	0.5053	3
6	0.0686	0.0459	0.4007	8
7	0.0538	0.0667	0.5537	1
8	0.0716	0.0541	0.4306	7
9	0.0638	0.0639	0.5003	4

**Table 12 - Mean value for Performance coefficient (Pi)**

<b>Input variables</b>	<b>Level of input variables</b>			<b>Delta = (Max-Min)</b>	<b>Optimal settings</b>	<b>Rank</b>
	<b>I</b>	<b>II</b>	<b>III</b>			
Nc	0.4615	0.4664	0.4949	0.0334	III	3
f	0.5199	0.4401	0.5154	0.0797	I	1
Vc	0.4480	0.4594	0.5154	0.0675	III	2

**Table 13 - Confirmation test result**

<b>Responses</b>	<b>Initial</b>	<b>Predicted</b>	<b>Optimal</b>
	<i>Nc1-f2-Vc2</i>	<i>Nc3-f1-Vc3</i>	<i>Nc3-f1-Vc3</i>
VBc(mm)	0.065		0.071
Ra ( $\mu\text{m}$ )	1.51		1.11
MRR (g/s)	0.000825		0.00089
Performance coefficient (Pi)	0.3845	0.5816	0.5537
Improvement in Pi		0.1692	

## 5. Conclusion

In the present research work, Incoloy 330 alloy was machined using TiAlN PVD coated cutting tool in turning operation using MQL technique where different concentrations of coconut oil-based SiO<sub>2</sub> Nanofluids were used as a lubricating agent to examine the effects of input process variables on flank wear, surface roughness, MRR, and chip morphology. TOPSIS optimization technique is used to optimize the multi responses and get an optimal process parameter for which the output parameter is significantly good.

- TiAlN PVD coated cemented carbide tool experienced lower width of flank wear (0.3 mm to 0.074 mm) due to effective lubrication capabilities of SiO<sub>2</sub> nanofluid and high Vickers hardness number and anti-adhesion characteristics of tool justify its use in machining hard to cut material like Incoloy 330 to achieve better tool life.
- Built-up-edge formation, abrasion, adhesion, micro-chipping as well as chipping mode of wear mechanisms on tool-tip are found in the current investigation.
- Surface quality is deteriorating with increasing feed rate. The highest feed rate (0.35 mm/rev) is not recommended to use for machining as Ra is noticed to be larger than the standard roughness limit of 1.6  $\mu\text{m}$ .
- With the increase in cutting speed and feed rate, MRR increases but at the same condition surface quality deteriorates. However, optimum cutting conditions are recommended for the MRR concern.
- Chips are found to be as a coiled continuous helical shape with a larger diameter which is easily removed from the cutting zone which reduces the friction and chip-tool interface temperature during machining. Chip

reduction coefficient decreases with feed and cutting speed while effects of nanofluid concentration are negligible while deformed chip-thickness increased with feed and reduced with cutting speed.

- TOPSIS optimization recommended the following settings of input terms:  $N_c$  (3<sup>rd</sup> level) = 0.3 %wt;  $f$  (1<sup>st</sup> level) = 0.15 mm/rev and  $V_c$  (3<sup>rd</sup> level) = 160 m/min. In this condition, the performance coefficient ( $P_i$ ) is improved by 40 % from the initial setting.

No machining works are available on the machinability study of Incoloy 330 alloy in previously published literature. Therefore, more research needs to be carried considering a different combinations of input variables (cutting speed, feed, and depth of cut), tool geometry, and machining environments. Distinguish response studies like micro structure of the finished surface, cutting force, cutting temperature, and residual stresses are recommended in the future. Application of innovative cooling techniques considering distinguish coolant/lubrication can be carried out to enhance the machinability aspects of Incoloy 330 alloy.

## Acknowledgement

Authors are grateful to KIIT, Deemed to be University to provide the necessary instruments and equipment's to carry out the current research.

## References

- [1] Choudhury, I. A., & El-Baradie, M. A. (1998). Machinability of nickel-base super alloys: a general review. *Journal of Materials Processing Technology*, 77(1-3), 278-284.
- [2] Ezugwu, E. O., Wang, Z. M., Machado, A. R. (1999). The machinability of nickel-based alloys: a review. *Journal of Materials Processing Technology*, 86(1-3), 1-16.
- [3] Yazid, M. Z. A., & Zainol, A. (2019). Environmentally Friendly Approaches Assisted Machining of Aluminum Alloy 7075-T6 for Automotive Applications: A Review. *International Journal of Integrated Engineering*, 11(6), (2019), 18-26.
- [4] Sani, A. S. A., Rahim, E. A., Sharif, S., & Sasahara, H. (2019). Machining performance of vegetable oil with phosphonium-and ammonium-based ionic liquids via MQL technique. *Journal of cleaner production*, 209, 947-964.
- [5] Ali, N., Teixeira, J. A., & Addali, A. (2018). A review on nanofluids: fabrication, stability, and thermophysical properties. *Journal of Nanomaterials*, <https://doi.org/10.1155/2018/6978130>.
- [6] Venkatesana, K., Devendiranb, S., Ghazaly, N. M., Rahuld, R., & Mughilane, T. (2019). Optimization of Cutting Parameters on turning of Incoloy 800H using  $Al_2O_3$  Nanofluid in Coconut oil. *Procedia Manufacturing*, 30, 268–275.
- [7] Musavi, S. H., Davoodi, B., & Niknam, S. A. (2019) Effects of reinforced nanoparticles with surfactant on surface quality and chip formation morphology in MQL-turning of superalloys. *Journal of Manufacturing Processes*, 40, 128-139.
- [8] Hegab, H., Darras, B., & Kishawy, H. A. (2018). Sustainability assessment of machining with nano-cutting fluids. *Procedia Manufacturing*, 26, 245-254.
- [9] Rahmati, B., Sarhan, A. A., & Sayuti, M. (2014). Investigating the optimum molybdenum disulfide (MoS<sub>2</sub>) nanolubrication parameters in CNC milling of AL6061-T6 alloy. *The International Journal of Advanced Manufacturing Technology*, 70(5-8), 1143-1155.
- [10] Weinert, K., Inasaki, I., Sutherland, J. W., & Wakabayashi, T. (2004). Dry machining and minimum quantity lubrication. *CIRP annals*, 53(2), 511-537.
- [11] Sreejith, P. S., & Ngoi, B. K. A. (2000). Dry machining: machining of the future. *Journal of materials processing technology*, 101(1-3), 287-291
- [12] Diniz, A. E., & Micaroni, R. (2002) Cutting conditions for finish turning process aiming: the use of dry cutting. *International Journal of Machine Tools and Manufacture*, 42(8), 899-904.
- [13] Khan, M. M. A., Mithu, M. A. H., & Dhar, N. R. (2009) Effects of minimum quantity lubrication on turning AISI 9310 alloy steel using vegetable oil-based cutting fluid. *Journal of materials processing Technology*, 209(15-16), 5573-5583.
- [14] Tiwari, A. K., Ghosh, P., Sarkar, J., Dahiya, H., & Parekh, J. (2014) Numerical investigation of heat transfer and fluid flow in plate heat exchanger using nanofluids. *International Journal of Thermal Sciences*, 85, 93-103.
- [15] Kumar, R., Sahoo, A. K., Mishra, P. C., & Das, R. K. (2018) Comparative investigation towards machinability improvement in hard turning using coated and uncoated carbide inserts: part I experimental investigation. *Advances in Manufacturing*, 6(1), 52-70.
- [16] Wang, X. Q., & Mujumdar, A. S. (2007). Heat transfer characteristics of nanofluids: a review. *International journal of thermal sciences*, 46(1), 1-19.
- [17] Wang, X. Q., & Mujumdar, A. S. (2008). A review on nanofluids-part I: theoretical and numerical investigations. *Brazilian Journal of Chemical Engineering*, 25(4), 613-630.

- [18] Hussein, A. K. (2015). Applications of nanotechnology in renewable energies - A comprehensive overview and understanding. *Renewable and Sustainable Energy Reviews*, 42, 460-476.
- [19] Sharma, A. K., Tiwari, A. K., & Dixit, A. R. (2016) Characterization of TiO<sub>2</sub>, Al<sub>2</sub>O<sub>3</sub> and SiO<sub>2</sub> nanoparticle based cutting fluids. *Materials Today: Proceedings*, 3(6), 1890-1898.
- [20] Das, A., Pradhan, O., Patel, S. K., Das, S. R., & Biswal, B. B. (2019) Performance appraisal of various nanofluids during hard machining of AISI 4340 steel. *Journal of Manufacturing Processes*, 46, 248-270.
- [21] Das, A., Patel, S. K., & Das, S. R. (2019) Performance comparison of vegetable oil based nanofluids towards machinability improvement in hard turning of HSLA steel using minimum quantity lubrication. *Mechanics & Industry*, 20(5), 506.
- [22] Das, A., Das, S. R., Patel, S. K., & Biswal, B. B. (2019) Effect of MQL and nanofluid on the machinability aspects of hardened alloy steel. *Machining Science and Technology*, DOI: 10.1080/10910344.2019.1669167.
- [23] Kumar, R., Sahoo, A. K., Mishra, P. C., & Das, R. K. (2019) Performance assessment of air-water and TiO<sub>2</sub> nanofluid mist spray cooling during turning hardened AISI D2 steel. *Indian Journal of Engineering and Materials Sciences*, 26, 235-253.
- [24] Lazarević, V. B., Krstić, I. M., Takić, L. M., Lazić, M. L., & Veljković, V. B. (2011). Clarification and filtration of the flocculated partucle suspension from a chemical treatment of waste oil-in-water emulsions from a non-ferrous metalworking plant. *Hemijaska industrija*, 65(1), 53-60.
- [25] Das, A., Tirkey, N., Patel, S. K., Das, S. R., & Biswal, B. B. (2019) A Comparison of Machinability in Hard Turning of EN-24 Alloy Steel Under Mist Cooled and Dry Cutting Environments with a Coated Cermet Tool. *Journal of Failure Analysis and Prevention*, 19(1), 115-130.
- [26] Sopian, N. F., Omar, B., & Abd Shukor, M. H. (2010) Integrated mechanical pulse jet coolant delivery system performance for minimal quantity lubrication. *International Journal of Integrated Engineering*, 2(1), 1-16.
- [27] Bouzakis, K. D., Michailidis, N., Skordaris, G., Bouzakis, E., Biermann, D., & M'Saoubi, R. (2012). Cutting with coated tools: Coating technologies, characterization methods and performance optimization. *CIRP annals*, 61(2), 703-723.
- [28] Hosokawa, A., Shimamura, K., & Ueda, T. (2012). Cutting characteristics of PVD-coated tools deposited by unbalanced magnetron sputtering method. *CIRP annals*, 61(1) 95-98.
- [29] Kumar, T. S., Prabu, S. B., & Kumar, T. S. (2016). Comparative evaluation on the performance of nanostructured TiAlN, AlCrN, TiAlN/AlCrN coated and uncoated carbide cutting tool on turning EN24 alloy steel, *Indian Journal of Engineering & Materials Sciences*, 23(1), 45-59.
- [30] Rakesh, M., & Datta, S. (2019). Effects of Cutting Speed on Chip Characteristics and Tool Wear Mechanisms During Dry Machining of Inconel 718 Using Uncoated WC Tool. *Arabian Journal for Science and Engineering*, 1-18.
- [31] Akhtar, W., Sun, J., Sun, P., Chen, W., & Saleem, Z. (2014). Tool wear mechanisms in the machining of Nickel based super-alloys: A review. *Frontiers of Mechanical Engineering*, 9(2), 106-119.
- [32] Hegab, H., Umer, U., Soliman, M., & Kishawy, H. A. (2018). Effects of nano-cutting fluids on tool performance and chip morphology during machining Inconel 718. *The International Journal of Advanced Manufacturing Technology*, 96(9-12), 3449-3458.
- [33] Kumar, R., Sahoo, A. K., Mishra, P. C., Panda, A., Das, R. K. & Roy, S. (2019) Prediction of machining performances in hardened AISI D2 steel, *Materials Today: Proceedings*, 18(7), 2486-2495.
- [34] Kumar, R., Sahoo, A. K., Mishra, P. C., Das, R. K. & Ukamanal, M. (2018). Experimental investigation on hard turning using mixed ceramic insert under accelerated cooling environment. *International Journal of Industrial Engineering Computations*, 9(4), 509-522.
- [35] Panda, A., Das, S.R., & Dhupal, D. (2018) Experimental investigation, modelling and optimization in hard turning of high strength low alloy steel (AISI 4340). *Matériaux & Techniques* 106(4), 404.
- [36] Kumar, R., Sahoo, A. K., Mishra, P. C., & Das, R. K. (2019). Measurement and machinability study under environmentally conscious spray impingement cooling assisted machining. *Measurement*, 135, 913-927
- [37] Abdulkareem, S., Rumah, U. J., & Adaokoma, A. (2011) Optimizing Machining Parameters during Turning Process. *International Journal of Integrated Engineering*, 3(1), 23-27
- [38] Marimuthu, P., & Baskaran, R. (2014). Optimal setting of machining parameters for turning Inconel 625 using coated tool. *Applied Mechanics and Materials*, 573, 632-637.
- [39] Angappan, P., Thangiah, S., & Subbarayan, S. (2017) Taguchi-based grey relational analysis for modeling and optimizing machining parameters through dry turning of Incoloy 800H. *Journal of Mechanical Science and Technology*, 31(9), 4159-4165.
- [40] Thakur, A., Gangopadhyay, S., Maity, K. P. & Sahoo, S. K. (2016) Evaluation on Effectiveness of CVD and PVD Coated Tools during Dry Machining of Incoloy 825, *Tribology Transactions*, 59(6), 1048-1058.
- [41] Bhatt, A., Attia, H., Vargas, R., & Thomson, V. (2010). Wear mechanisms of WC coated and uncoated tools in finish turning of Inconel 718. *Tribology International*, 43(5-6), 1113-1121.
- [42] Talib, N., Md Nasir, R., & Abd Rahim, E. (2018) Investigation on the Tribological Behaviour of Modified Jatropa Oil with Hexagonal Boron Nitride Particles as a Metalworking Fluid for Machining Process. *International Journal of Integrated Engineering*, 10(3), 57-62.

- [43] Balasubramanian, S., & Selvaraj, T. (2016). Application of integrated Taguchi and TOPSIS method for optimization of process parameters for dimensional accuracy in turning of EN25 steel. *Journal of the Chinese Institute of Engineers*, 40(4), 267-274.
- [44] Balioti, V., Tzimopoulos, C., & Evangelides, C. Multi-Criteria Decision Making Using TOPSIS Method Under Fuzzy Environment. Application in Spillway Selection. In *Multidisciplinary Digital Publishing Institute Proceedings*, vol. 2: (2018) 637.
- [45] Parida, A. K., & Routara, B. C. (2014). Optimization of process parameters in turning of GFRP using TOPSIS method. *International scholarly research notices*, <http://dx.doi.org/10.1155/2014/905828>
- [46] Ramesh, S., Viswanathan, R., & Ambika, S. (2016). Measurement and optimization of surface roughness and tool wear via grey relational analysis, TOPSIS and RSA techniques. *Measurement*, 78, 63-72.